High frequency operation of an integrated electro-absorption modulator onto a VCSEL

Ludovic Marigo-Lombart, Alexandre Rumeau, Christophe Viallon, Alexandre Arnoult, Stéphane Calvez, Antoine Monmayrant, Olivier Gauthier-Lafaye, R Rosales, J A Lott, H Thienpont, et al.

High frequency operation of an integrated electro-absorption modulator onto a VCSEL

L Marigo-Lombart[1,3], A Rumeau[1], C Viallon[1], A Arnoult[1], S Calvez[1], A Monmayrant[1], O Gauthier-Lafaye[1], R Rosales[2], JA Lott[2], H Thienpont[3], K Panajotov[3] and G Almuneau[1]

[1]LAAS-CNRS, Université de Toulouse, CNRS, Toulouse, France

[2]Center of Nanophotonics, Institute of Solid-State Physics, Technische Universität Berlin , Berlin D-10623, Germany

[3]Department of Applied Physics and Photonics (TW-TONA), Vrije Universiteit Brussel, Pleinlaan 2, B-1050 Brussels, Belgium

E-mail: `almuneau@laas.fr`

July 2018

Abstract. We present in this paper the vertical integration of an electro-absorption modulator (EAM) onto a VCSEL. We discuss the design, fabrication, and measured characteristics of the combined VCSEL and EAM. We previously demonstrated a standalone EAM with an optical bandwidth around 30 GHz. In this paper we present for the first time an optical bandwidth of 30 GHz for an electro-absorption modulator integrated onto a VCSEL. This device exhibits single-mode operation and a very low chirp, below 0.1 nm, even with a modulation depth of 70 % which makes this device very competitive for high-speed communications in data centers.

Submitted to: *J. Phys. : Photonics*

1. Introduction

Nowadays, Vertical-Cavity Surface-Emitting Lasers (VCSELs) receive a lot of attention for their versatility in different emerging applications requiring massively expanding data transmission rates. In particular, in very recent years, new applications including internet of things (IoT), virtual reality, cloud computing and storage, have driven the demand for a significant expansion in capacity of short-reach links in data centers [1], favouring solutions with low power consumption. In that context, VCSELs bring many advantages to optical transceivers, such as a high density of integration and an easy coupling to optical fibers, making them ideal as light sources for very high-frequency and high-capacity data links.

Direct modulation on short wavelength VCSELs (850, 940 or 980 nm) has been greatly improved through many device design strategies, but the performances are restricted by different intrinsic physical limitations including carrier-photon dynamics, parasitic electrical losses, and self-heating. Albeit, VCSELs with impressive performances have been demonstrated in the past years reaching modulation frequencies in excess of 25 GHz [2] [3] [4]. In particular, VCSELs with very small oxide confinement apertures (down to few micrometers in diameter) have been found to increase the modulation bandwidth to above 30 GHz [5], but at the expense of a very stringent fabrication which is not entirely compatible with high volume manufacturing on 4-inch, or even 6-inch-diameter wafers. Nevertheless, using directly-modulated devices with complex but more efficient modulation formats such PAM-4 or Discrete MultiTone (DMT) has enabled optical data systems to reach transmission rates in the range of 100 Gbps on single channel links [6] [7] [8].

In order to reach even higher communication speeds, the configuration based on externally modulated laser (EML) is more adapted and advantageous as established in long and medium-range links with systems exploiting distributed feedback lasers (DFB) that are in-wafer-plane integrated with an EAM. The implementation of such EML with VCSEL sources would allow their respective inherent advantages to be combined and enable very high speed data transfers with low power consumption to be obtained.

Despite these potential benefits, such a vertical EML configuration has been scarcely studied and developed to-date. In fact, the co-integration of VCSELs with an electro-optic modulator has been proposed by several groups by combining them laterally [9] or vertically in an integrated monolithic device. In this last configuration two solutions are possible. The first one is by modulating the refractive index of the top distributed Bragg reflector (DBR), and so the reflectivity spectrum via an electric field (based on the electro-refractive effect (ER)) [10]. In that case, both cavities are strongly coupled which allows very high bandwidth at the expense of a high chirp and a low transmission data rate. **(high bandwidth and low data rate?!!!)** The second one, based on the absorption modulation induced by the quantum-confined Stark effect, in which case the two optical cavities are weakly coupled and where high-frequency modulation with regulated temperature has already achieved [11].

About the ER modulator, the first idea developed by Avrutin [12] has been then implemented by Chang-Hasnain's team at the University of California, Berkeley, by incorporating an intra cavity quantum well absorber within the VCSEL, more precisely in the top DBR. By applying a voltage, the mirror reflectivity changes and so does the laser output power [13]. However, this technique showed lower modulation speed (9 GHz) than direct VCSEL modulation. Also, the splitting of the modulating and the emitting part could avoid the carrier dynamics limitation.

A demonstration of a composite-resonator VCSEL has been reported by Chen et al. [14] where both cavities are current-modulated. The total output power is thus the superposition of the contributions of the two (laser) cavities. Another device concept, demonstrated in 2012 [15], comprises an electro-optical modulator on top of the VCSEL with both cavities having similar resonance wavelengths when the modulator section is subjected to a significant electric field of several tens of volts. Unfortunately, due to the coupling between both cavities, the emission wavelength is affected by the modulation resulting in a wavelength shift of about 1.5 nm [16] [17]. To avoid this chirp and decrease the required voltage, the electro-absorption phenomenon can be preferably used, as done by Van Eisden in 2008 [18]. A modulation at 20 GHz was demonstrated by proper detuning of the EAM and VCSEL cavity resonances. The idea of an external modulation is also interesting to increase the device lifetime which is degraded by the high drive current.

Higher bandwidths could be achieved if the parasitic capacitances and resistances are further reduced. Temperature control is also a challenge to preserve low power consumption and a reduced chirp size. The development of these two last points have been the main items of our work and will be presented in this paper.

We present in this paper a device based on the proposed concept of Van Eisden et al., the vertical integration of an electro-absorption modulator onto a VCSEL. We describe in the first section the structure description and the fabrication of this three electrode device. Then we demonstrate the efficiency of this device with static characterization. Finally, the high-frequency modulation results will be discussed.

2. Structure description and fabrication

The EAM VCSEL structure has been grown, with an N-P-N doping profile, monolithically in one single epitaxial run on an N-doped GaAs substrate on a RIBER 412 molecular beam epitaxy (MBE) system.

Above the substrate, the structure combines a conventional 850 nm VCSEL structure stacked with an asymmetric Fabry-Perot modulator (AFPM) structure.

The VCSEL part is formed by a 35.5 period $Al_{0.9}GaAs/Al_{0.15}GaAs$ N-type bottom distributed Bragg reflector (DBR), a half-wave thick optical cavity including three $GaAs/Al_{0.3}GaAs$ quantum well/barrier layers (QW), and a 12.5 periods P-type DBR embedding an $Al_{0.98}GaAs$ 30 nm-thick layer for oxide confinement in the first period above the cavity. Above that, a P-type $3\lambda/4$-thick layer is grown to serve commonly as the top-electrode of the VCSEL and the bottom-electrode of the EAM. Above, the AFPM structure is grown composed of a 10.5-period P-doped DBR (with the same composition as used in the VCSEL's DBRs), a 2λ-thick undoped cavity embedding 25 $GaAs/Al_{0.3}GaAs$ QWs, and finally capped by an N-doped 6.5-period DBRs and a 50 nm GaAs cap as an N-contact layer.

The common intermediate DBR was deliberatly thick enough (23 periods overall) to minimize the coupling between the VCSEL cavity and the EAM cavity to reduce the impact of the coupled vertical cavities on optical feedback that may impact the VCSEL performance while enabling good modulation. Also, a not too high top mirror reflectivity as seen by photons in the VCSEL cavity have to be kept to not decrease the output power.

The second crucial point is the wavelength detuning between the VCSEL cavity (respectively AFPM cavity) resonance and the VCSEL gain (resp. AFPM QWs absorption tail) to ensure large temperature range operation. Typically a redshift room temperature cavity detuning of about 15 nm with respect to the QW photoluminescence peak leads to a perfect gain-to-cavity alignment around 40-50°C, when the integrated AFPM undergoes about the same heating as the VCSEL.

Furthermore the VCSEL and AFPM cavity resonances are slightly offset to avoid optical feedback between both cavities, as shown in [18].

Following the epitaxial growth of the EAM VCSEL structure, the respective wavelength detunings were measured by top reflectivity and photoluminescence (PL) on the global epitaxial structure and after successive etching steps down to atop the EAM and the VCSEL cavities. The measured cavity to peak PL offsets are +23 and +22 nm respectively for the VCSEL and the EAM, while the the VCSEL cavity resonance is redshifted by 5 nm compared to the EAM cavity resonance wavelength.

Then, the technological fabrication of the devices was realized by implementing triple contact electrodes for biasing independently the VCSEL and the EAM. Also, for high frequency (HF) operation, we applied a BCB planarization process overlaying the whole 6 μm-thick EAM VCSEL, and a low loss microstrip injection scheme for the modulator section. The details of the processing steps for the BCB planarization using an original pressing techniques and a HF pad design will be published elsewhere [19].

The final realized device is schematized on Fig. 1. For clarity, only vertical dimensions are to scale, as the horizontal dimensions are foreshortened.

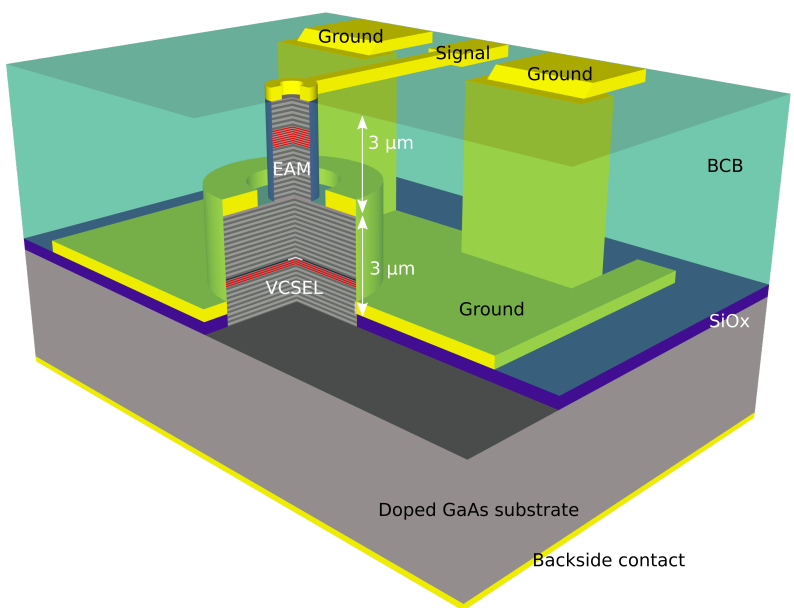

Figure 1. Global view of the fabricated EAM VCSEL device with microstrip line access for RF signal injection

3. EAM VCSEL static characterization

The Fig. 2 presents the light-current (LI) response of the VCSEL while applying different static voltages to the modulator section at room temperature.

In Fig. 2 a) the modulation effect can clearly be seen on the LI curve without any significant change of the lasing threshold current proving the decoupled operation of both cavities. The demonstrated modulation depth shown in Fig. 2 b) reaches 70% for a voltage change of 10 V across the EAM, for a driving current just above the VCSEL threshold. We can note that a modulation depth surpassing 40% can be reached all over the LI curve, showing that the modulation can be applied for any values of the output power from the VCSEL.

The optical spectra have also been measured with an optical spectrum analyser (OSA) as shown in Fig. 2 c), for different VCSEL currents and different voltages on the EAM. A redshift of the laser emission is observed when the driving current rises according to the inherent temperature increase in the structure. Whereas, at a given injected current the wavelength remains stable when a voltage is applied on the EAM ((for example as can be seen in Fig. 2d)). The maximum wavelength chirp of 80 pm is observed when a modulation depth of 70% is applied.

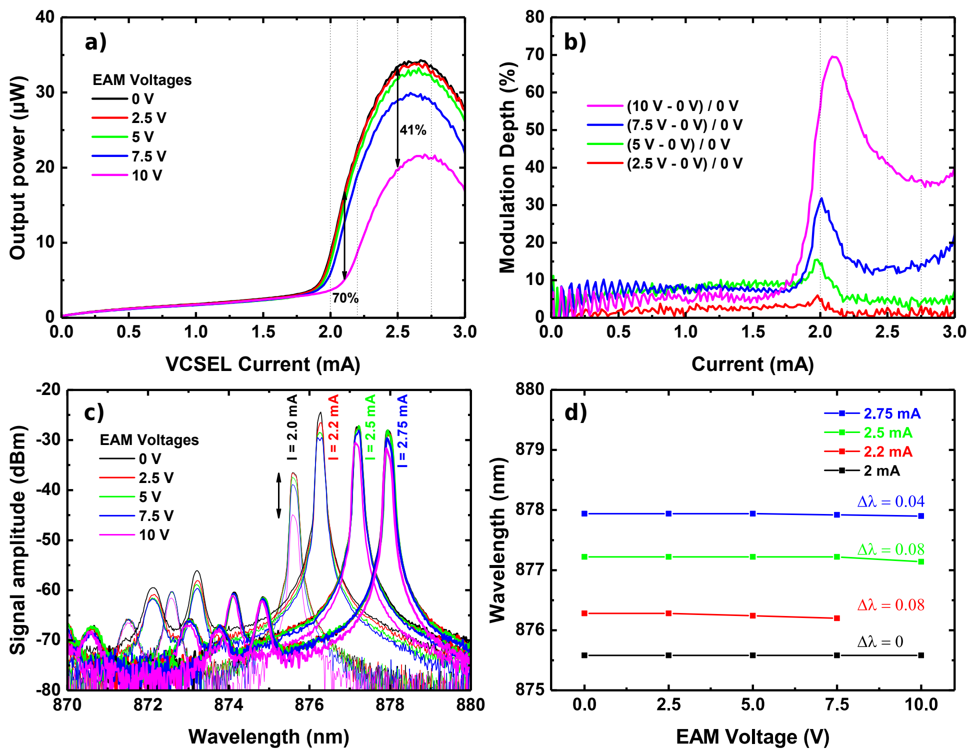

Figure 2. (a) L-I curve of the EAM VCSEL structure at room temperature. The output power is plotted for different EAM voltages. (b) is the modulation depth function of the applied EAM voltage. (c) Emission spectra under different EAM bias voltages. (d) Extraction of the wavelength shift when the VCSEL is modulated

4. EAM VCSEL high frequency modulation

Discrete standalone EAM structures were first characterized by measuring the top reflectivity at a fixed wavelength through a cleaved single-mode fiber tip, while the HF voltage signal was injected with a cascade Infinity 67 GHz GSG-150 probe. A tunable laser source was used as a monochromatic illumination source on the top of the EAM, and a fiber coupler enabled the collection of the reflected signal. A FieldFox Keysight was used to extract the EAM frequency response through a high-speed photodiode. Details of this measurement setup is given in [20]. The EAM standalone vertical modulators exhibit modulation bandwidths in the range of 28-32 GHz respectively for modulator diameters from 26 to 18 μm.

Also for HF characterizations of both the EAM and the EAM VCSEL structures, the injection losses due the different RF elements in the setup were carefully characterized and compensated in order to retrieve the real input and output powers to/from the studied modulator devices [20]. In particular, the frequency response of the New Focus 1434 InGaAs photodetector used for the measurements was measured by a heterodyne technique for an 850 nm wavelength giving a f_{-3dB} of 27 GHz, and hence the measured response could be considered for extracting the effective modulation amplitude of the EAM up to 40 GHz.

The EAM VCSELs were next characterized with an HF voltage applied to the EAM terminals with a VNA Agilent PNA-X 67 GHz. The presented results have been measured on a 71 μm diameter VCSEL, with an oxide aperture diameter of less than 5 μm, topped with a 24 μm EAM. The normalized frequency response of the EAM VCSEL devices is shown on Fig. 3 with an applied current of 2.9 mA on the VCSEL section and a DC bias of 8.5 V on the EAM. The injected modulated voltage amplitude is estimated to be < 1 V in the full range of frequencies due to the limited power delivered by the VNA and the high impedance of the EAM itself. In agreement with the previous results on a standalone EAM, a -3dB modulation bandwith as high as 29 GHz has been measured. This result shows clearly the advantage of decoupling the modulator section from the VCSEL emitter, and indeed the potential gain compared to directly modulated VCSELs. For comparison, these results show a significant improvement compared to the results from [18] on an equivalent EAM VCSEL structure. This last structure contains a thicker intermediate DBR separating the two cavities, and multiple double QWs which serves as the modulated absorbing region. Regarding the HF injection configuration, our design seems to be more optimized in terms of reduced HF injection losses, including the use of a 2-λ thick cavity for reducing the device capacitance compared to a 1.5-λ-thick cavity.

The frequency response of the EAM/VSEL device was also studied at different EAM DC bias, in order to check the influence of the working point on the absorption curve on the dynamics (in Fig. 4). As already reported in [11], the DC bias applied on the modulator modifies noticeably the shape of the frequency response. In particular, a strong resonance peak arises around 3 GHz, and is strongly dependent on the bias voltage. In the inset of Fig. 4 we plotted this relaxation frequency against the bias voltage on the EAM. When increasing the bias, this peak goes to a minimum frequency at 2.5 GHz while decreasing in intensity, until it vanishes for a bias of 8.5 V, for which the frequency response is flat up to 20 GHz. For higher values of the bias, the resonance

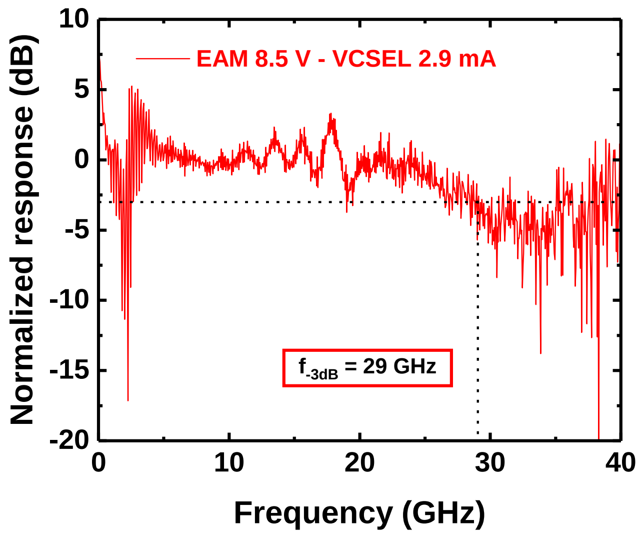

Figure 3. Modulation frequency response at room temperature of the EAM VCSEL. The VCSEL is powered at 2.9 mA and the EAM at 8.5 V.

peak arises again, and its frequency increases again towards the same frequency observed at low biases.

This evolution has been explained by Van Eisden [11] as an additional modulation of the mirror reflectivity which in-turn impacts the photon density in the laser cavity, giving rise to a relaxation resonance frequency. Nevertheless, this resonance can be avoided by tuning accordingly the EAM bias, and then to significantly increase the modulation bandwidth.

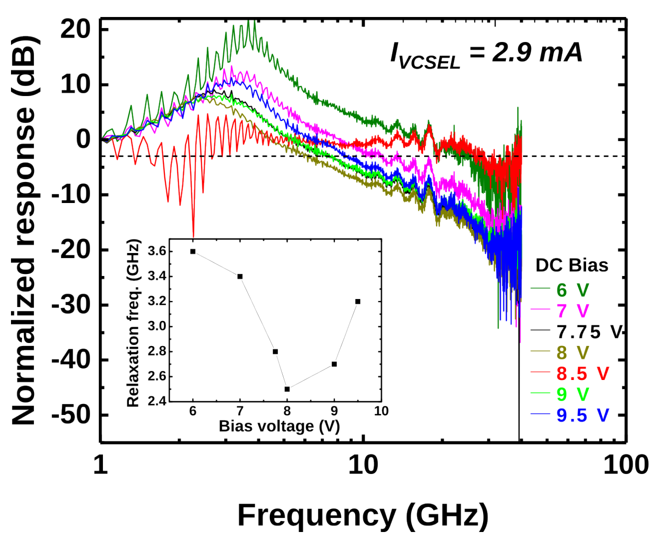

Figure 4. Modulation frequency response at room temperature of the EAM VCSEL under different DC bias on the EAM section. Inset : Frequency of the resonance peak around 3 GHz as the function of the EAM bias

Conclusions

We have demonstrated the fabrication and the characterization of a new monolithic configuration of an EAM VCSEL, in which the gain and the modulation cavity resonances are optically decoupled. The effective modulation through an AFPM based on electro-absorption allows us to achieve a large modulation contrast while ensuring a very small wavelength chirp compared to devices that operate via the electro-refractive effect. The fabrication of the EAM VCSEL device has been realized with a low loss RF injection microstrip line access and properly planarized thick BCB layer. The high-frequency modulation on this EAM VCSEL device has been successfully demonstrated up to 29 GHz with a flat response through the adjustment of the applied bias on the modulator. This modulation bandwidth is to our knowledge the best achieved on this type of electro-absorption modulated VCSEL.

Acknowledgments

The authors gratefuly acknowledge the technological support of RENATECH (French Network of Technology Platforms) within the LAAS-CNRS cleanroom infrastructure and the financial support of the Methusalem foundation, Belgium.

References

[1] K. Zhong, X. Zhou, J. Huo, C. Yu, C. Lu, and A. P. T. Lau, “Digital signal processing for short-reach optical communications: A review of current technologies and future trends,” *Journal of Lightwave Technology*, vol. 36, no. 2, pp. 377–400, jan 2018.

[2] E. Haglund, A. Larsson, M. Geen, J. S. Gustavsson, E. P. Haglund, A. Joel, and P. Westbergh, “30 GHz bandwidth 850 nm VCSEL with sub-100 fJ/bit energy dissipation at 25–50 gbit/s,” *Electronics Letters*, vol. 51, no. 14, pp. 1096–1098, jul 2015.

[3] W. Hamad, S. Wanckel, and W. H. E. Hofmann, “Small-signal analysis of ultra-high-speed multi-mode VCSELs,” *IEEE Journal of Quantum Electronics*, vol. 52, no. 7, pp. 1–11, jul 2016.

[4] M. Feng, C.-H. Wu, and N. Holonyak, “Oxide-confined VCSELs for high-speed optical interconnects,” *IEEE Journal of Quantum Electronics*, vol. 54, no. 3, pp. 1–15, jun 2018.

[5] R. Rosales, M. Zorn, and J. A. Lott, “30-GHz bandwidth with directly current-modulated 980-nm oxide-aperture VCSELs,” *IEEE Photonics Technology Letters*, vol. 29, no. 23, pp. 2107–2110, dec 2017.

[6] D. M. Kuchta, A. V. Rylyakov, F. E. Doany, C. L. Schow, J. E. Proesel, C. W. Baks, P. Westbergh, J. S. Gustavsson, and A. Larsson, “A 71-gb/s NRZ modulated 850-nm VCSEL-based optical link,” *IEEE Photonics Technology Letters*, vol. 27, no. 6, pp. 577–580, mar 2015.

[7] C. Kottke, C. Caspar, V. Jungnickel, R. Freund, M. Agustin, J. R. Kropp, and N. N. Ledentsov, “High-speed DMT and VCSEL-based MMF transmission using pre-distortion,” *Journal of Lightwave Technology*, vol. 36, no. 2, pp. 168–174, jan 2018.

[8] J. Chen, Z. S. He, T. Lengyel, K. Szczerba, P. Westbergh, J. S. Gustavsson, H. Zirath, and A. Larsson, “An energy efficient 56 gbps PAM-4 VCSEL transmitter enabled by a 100 gbps driver in 0.25 μm InP DHBT technology,” *Journal of Lightwave Technology*, vol. 34, no. 21, pp. 4954–4964, nov 2016.

[9] X. Gu, M. Nakahama, A. Matsutani, M. Ahmed, A. Bakry, and F. Koyama, “850 nm transverse-

coupled-cavity vertical-cavity surface-emitting laser with direct modulation bandwidth of over 30 ghz," *Applied Physics Express*, vol. 8, no. 8, p. 082702, 2015.

[10] T. D. Germann, A. Strittmatter, A. Mutig, A. M. Nadtochiy, J. A. Lott, S. A. Blokhin, L. Y. Karachinsky, V. A. Shchukin, N. N. Ledentsov, U. W. Pohl, and D. Bimberg, "Monolithic electro-optically modulated vertical cavity surface emitting laser with 10 gb/s open-eye operation," *physica status solidi (c)*, vol. 7, no. 10, pp. 2552–2554, 2010.

[11] J. van Eisden, M. Yakimov, V. Tokranov, M. Varanasi, E. M. Mohammed, I. A. Young, and S. R. Oktyabrsky, "Optically decoupled loss modulation in a duo-cavity VCSEL," *IEEE Photonics Technology Letters*, vol. 20, no. 1, pp. 42–44, 2008.

[12] E. A. Avrutin, V. B. Gorfinkel, S. Luryi, and K. A. Shore, "Control of surface-emitting laser diodes by modulating the distributed bragg mirror reflectivity: Small-signal analysis," *Applied Physics Letters*, vol. 63, no. 18, pp. 2460–2462, nov 1993.

[13] J. Hudgings, R. Stone, C.-H. Chang, S. Lim, K. Lau, and C. Chang-Hasnain, "Dynamic behavior and applications of a three-contact vertical-cavity surface-emitting laser," *IEEE Journal of Selected Topics in Quantum Electronics*, vol. 5, no. 3, pp. 512–519, 1999.

[14] C. Chen, P. O. Leisher, C. Long, D. M. Grasso, and K. D. Choquette, "High-speed electroabsorption modulation of composite-resonator vertical-cavity lasers," *IET optoelectronics*, vol. 3, no. 2, pp. 93–99, 2009.

[15] T. D. Germann, W. Hofmann, A. M. Nadtochiy, J.-H. Schulze, A. Mutig, A. Strittmatter, and D. Bimberg, "Electro-optical resonance modulation of vertical-cavity surface-emitting lasers," *Optics express*, vol. 20, no. 5, pp. 5099–5107, 2012.

[16] V. A. Shchukin, N. N. Ledentsov, J. A. Lott, H. Quast, F. Hopfer, L. Y. Karachinsky, M. Kuntz, P. Moser, A. Mutig, A. Strittmatter, V. P. Kalosha, and D. Bimberg, "Ultra high-speed electro-optically modulated VCSELs: modeling and experimental results," in *Physics and Simulation of Optoelectronic Devices XVI*, M. Osinski, F. Henneberger, and K. Edamatsu, Eds. SPIE, feb 2008.

[17] A. Paraskevopoulos, H. J. Hensel, W. D. Molzow, H. Klein, N. Grote, N. N. Ledentsov, V. A. Shchukin, C. Moller, A. R. Kovsh, D. A. Livshits, I. L. Krestnikov, S. S. Mikhrin, P. Matthijsse, and G. Kuyt, "Ultra-high-bandwidth (>35 ghz) electrooptically-modulated VCSEL," in *2006 Optical Fiber Communication Conference and the National Fiber Optic Engineers Conference*. IEEE, 2006.

[18] M. Yakimov, J. van Eisden, V. Tokranov, M. Varanasi, S. R. Oktyabrsky, E. M. Mohammed, and I. A. Young, "Concept of feedback-free high-frequency loss modulation in detuned duo-cavity vertical cavity surface-emitting laser," *Journal of Vacuum Science & Technology B, Nanotechnology and Microelectronics: Materials, Processing, Measurement, and Phenomena*, vol. 28, no. 3, pp. C3G32–C3G37, may 2010.

[19] L. Marigo-Lombart, C. Viallon, A. Rumeau, A. Arnoult, A. Lecestre, L. Mazenq, A. Ghannam, H. Thienpont, K. Panajotov, and G. Almuneau, "High-speed electrical injection for electro-absorption modulator vertically integrated on a VCSEL using low permittivity BCB," *Submitted to IEEE Journal of Lightwave Technologies.*

[20] L. Marigo-Lombart, C. Viallon, A. Rumeau, O. Gauthier-Lafaye, A. Monmayrant, H. Thienpont, K. Panajotov, and G. Almuneau, "High frequency characterization of a vertical electro-absorption modulator for data communications," IEEE, Ed. International Topical Meeting on Microwave Photonics, 2018.